Plasmon-assisted optical trapping and anti-trapping

Aliaksandra Ivinskaya[1], Mihail I. Petrov[1], Andrey A. Bogdanov[1], Ivan Shishkin[2], Pavel Ginzburg[1,2] and Alexander S. Shalin[1,3,4,†]

Supplementary Information

Table of content

---

[1]Department of Nanophotonics and Metamaterials, ITMO University, Birzhevaja line, 14, 199034 St. Petersburg, Russia

[2]School of Electrical Engineering, Tel Aviv University, Ramat Aviv, Tel Aviv 69978, Israel

[3]Kotel'nikov Institute of Radio Engineering and Electronics of Russian Academy of Sciences (Ulyanovsk branch), Goncharova str. 48/2, 432071 Ulyanovsk, Russia

[4]Ulyanovsk State University, Lev Tolstoy str. 42, 432017 Ulyanovsk, Russia

†Correspondence: AS Shalin, E-mail: alexandesh@gmail.com

A. Green's function

The field produced by a point dipole is the sum of free-space Green's function and Green's function describing the field reflected from the substrate. Precisely at the dipole location $\mathbf{r}_0=(0,0,z)$ we have only the reflected field with Green's tensor taking the diagonal form:

$$\hat{\mathbf{G}}(\mathbf{r}_0,\mathbf{r}_0)=\frac{i}{8\pi}\int_0^\infty k_\rho\begin{bmatrix}\frac{r_s}{k_{z_1}}-\frac{r_p}{k_1^2} & & \\ & \frac{r_s}{k_{z_1}}-\frac{r_p}{k_1^2} & \\ & & \frac{2r_p k_\rho^2}{k_1^2 k_{z_1}}\end{bmatrix}\mathrm{e}^{-2ik_{z_1}z}\,\mathrm{dk}_\rho\,. \tag{S1}$$

The expressions for the derivatives are:

$$\partial_x\hat{\mathbf{G}}(\mathbf{r}_0,\mathbf{r}_0)=\frac{i}{8\pi k_1^2}\int_0^\infty r_p k_\rho^3\begin{bmatrix}0 & 0 & 1\\ 0 & 0 & 0\\ -1 & 0 & 0\end{bmatrix}\mathrm{e}^{-2ik_{z_1}z}\,\mathrm{dk}_\rho\,, \tag{S2}$$

$$\partial_z\hat{\mathbf{G}}(\mathbf{r}_0,\mathbf{r}_0)=-ik_{z_1}\hat{\mathbf{G}}(\mathbf{r}_0,\mathbf{r}_0)\,. \tag{S3}$$

In the last equation k_{z1} is supposed to be included in the integrand. The following notation is used in Equations (S1)-(S3): k_1 and k_2 are the wave vectors of incident radiation in the upper and lower half-spaces, k_ρ is the transverse component of the wave vector and $k_{z_1}=(k_1^2-k_x^2)^{1/2}$ and $k_{z_2}=(k_2^2-k_x^2)^{1/2}$ are normal to the interface components of the wave vectors in the two media. Amplitude reflection coefficients are

$$r_p=\frac{\varepsilon_2 k_{z_1}-\varepsilon_1 k_{z_2}}{\varepsilon_2 k_{z_1}+\varepsilon_1 k_{z_2}},\qquad r_s=\frac{k_{z_2}-k_{z_1}}{k_{z_2}+k_{z_1}}\,. \tag{S4}$$

By setting integration limits to $k_\rho= k_1$ in (S1)-(S3), evanescent waves scattered by the particle are excluded from the model and hence plasmon excitation does not take place.

B. Self-consistent field

In order to find the self-consistent field in the case of a dipolar scatterer, response of an auxiliary structure both to external illumination and to a point source situated at the location of the particle should be evaluated. Field produced by a particle with a dipole moment $\mathbf{p}$ positioned at $\mathbf{r}_0$ and oscillating at the frequency ω can be written as $\mathbf{E}^D(\mathbf{r}) = \omega^2 \mu_1 \mu_0 \hat{\mathbf{G}}(\mathbf{r},\mathbf{r}_0)\mathbf{p}$, where μ_1 and μ_0 are the medium and the vacuum permeability.

Having found a field without a scatterer and Green's tensor of the structure, we add the particle to the system. A dipole moment induced on the particle is given by $\mathbf{p} = \alpha \mathbf{E}(\mathbf{r}_0)$ while the self-consistent field is $\mathbf{E}(\mathbf{r}) = \tilde{\mathbf{E}}^{\mathbf{0}}(\mathbf{r}) + \mathbf{E}^{\mathbf{D}}(\mathbf{r})$. Now it is possible to derive $\mathbf{E}(\mathbf{r}_0)$ at the particle location explicitly and then obtain the general expression for the total field $\mathbf{E}(\mathbf{r}_0)$ at an arbitrary coordinate.

The total field in the particle-substrate system is a sum of initial field and the field scattered by the particle:

$$\mathbf{E}(\mathbf{r}) = \tilde{\mathbf{E}}^0(\mathbf{r}) + \mathbf{E}^D(\mathbf{r}) = \tilde{\mathbf{E}}^0(\mathbf{r}) + \omega^2 \mu_1 \mu_0 \hat{\mathbf{G}}(\mathbf{r},\mathbf{r}_0)\alpha \mathbf{E}(\mathbf{r}_0)\,. \tag{S5}$$

Self-consistent field at the dipole position is a solution of self-consistent Equation (S5) evaluated at $\mathbf{r}_0$:

$$\mathbf{E}(\mathbf{r_0}) = \frac{\tilde{\mathbf{E}}^{\mathbf{0}}(\mathbf{r_0})}{1 - \omega^2 \mu_1 \mu_0 \hat{\mathbf{G}}(\mathbf{r_0},\mathbf{r_0})\alpha}\,. \tag{S6}$$

After substituting (S6) to (S5), the total field is simply written as

$$\mathbf{E}(\mathbf{r}) = \tilde{\mathbf{E}}^0(\mathbf{r}_0)\left(1 + \frac{\omega^2 \mu_1 \mu_0 \hat{\mathbf{G}}(\mathbf{r},\mathbf{r}_0)\alpha}{1 - \omega^2 \mu_1 \mu_0 \hat{\mathbf{G}}(\mathbf{r}_0,\mathbf{r}_0)\alpha}\right). \tag{S7}$$

Differentiation of (S5) gives field derivatives

$$\partial_j \mathbf{E}(\mathbf{r}) = \partial_j \tilde{\mathbf{E}}_0(\mathbf{r}) + \omega^2 \mu_1 \mu_0 \partial_j \hat{\mathbf{G}}(\mathbf{r},\mathbf{r}_0)\alpha \mathbf{E}(\mathbf{r}_0)\,, \tag{S8}$$

where j is one of the coordinates. Since field derivatives are sums of two terms, two summands appear in the expression for the force:

$$F_j = \frac{1}{2}\Re(\alpha \mathbf{E}\partial_j \tilde{\mathbf{E}}^{0*}) + \frac{1}{2}|\alpha|^2 \omega^2 \mu\mu_0 \Re(\mathbf{E}\partial_j \hat{\mathbf{G}}^* \mathbf{E}^*) . \tag{S9}$$

From Equation (S7) the effective polarizability (satisfying $\mathbf{p} = \alpha\mathbf{E}(\mathbf{r}_0) = \hat{\alpha}^{eff}\tilde{\mathbf{E}}^0(\mathbf{r}_0)$) for diagonal Green's tensor can be derived as

$$\alpha_{jj}^{eff} = \frac{\alpha}{1-\omega^2\mu_1\mu_0 G_{jj}(\mathbf{r_0},\mathbf{r_0})\alpha} \tag{S10}$$

with particle polarizability

$$\alpha = \frac{\alpha_{ES}}{1 - i\dfrac{k_1^3}{6\pi\varepsilon_0}\alpha_{ES}}, \qquad \alpha_{ES} = 4\pi R^3 \varepsilon_0 \frac{\varepsilon-\varepsilon_1}{\varepsilon+2\varepsilon_1}, \tag{S11}$$

where ε_0 is the open space permittivity.

C. Force calculation

Horizontal and vertical forces for p-polarized Gaussian beam can be written as

$$\begin{aligned} F_x &= \frac{1}{2}\Re(\alpha E_x \partial_x E_x^* + \alpha E_z \partial_x E_z^*), \\ F_z &= \frac{1}{2}\Re(\alpha E_x \partial_z E_x^* + \alpha E_z \partial_z E_z^*). \end{aligned} \tag{S12}$$

Taking into account that Green's tensor is diagonal at the particle location $\mathbf{r_0}$, the total field on a dipole will have the same components as initial field $\tilde{\mathbf{E}}^0(\mathbf{r}_0)$:

$$E_x(\mathbf{r}_0) = \frac{\tilde{E}_x^0(\mathbf{r}_0)}{1-\omega^2\mu_1\mu_0 G_{xx}(\mathbf{r_0},\mathbf{r_0})\alpha}, \quad E_z(\mathbf{r}_0) = \frac{\tilde{E}_z^0(\mathbf{r}_0)}{1-\omega^2\mu_1\mu_0 G_{zz}(\mathbf{r_0},\mathbf{r_0})\alpha} . \tag{S13}$$

Field derivatives read

$$
\begin{aligned}
\partial_x E_x(\mathbf{r}_0) &= \partial_x \tilde{E}_x^0(\mathbf{r}_0) + \omega^2 \mu_1 \mu_0 \partial_x G_{xz}(\mathbf{r_0},\mathbf{r_0}) \alpha E_z(\mathbf{r}_0), \\
\partial_x E_z(\mathbf{r}_0) &= \partial_x \tilde{E}_z^0(\mathbf{r}_0) + \omega^2 \mu_1 \mu_0 \partial_x G_{zx}(\mathbf{r_0},\mathbf{r_0}) \alpha E_x(\mathbf{r}_0), \\
\partial_z E_x(\mathbf{r}_0) &= \partial_z \tilde{E}_x^0(\mathbf{r}_0) + \omega^2 \mu_1 \mu_0 \partial_z G_{xx}(\mathbf{r_0},\mathbf{r_0}) \alpha E_x(\mathbf{r}_0), \\
\partial_z E_z(\mathbf{r}_0) &= \partial_z \tilde{E}_z^0(\mathbf{r}_0) + \omega^2 \mu_1 \mu_0 \partial_z G_{zz}(\mathbf{r_0},\mathbf{r_0}) \alpha E_z(\mathbf{r}_0).
\end{aligned} \tag{S14}
$$

This gives us a full set of variables to find forces:

$$
\begin{aligned}
F_x &= \frac{1}{2}\Re(\alpha \mathbf{E} \partial_x \tilde{\mathbf{E}}^{0*}) + |\alpha|^2 \omega^2 \mu_1 \mu_0 \,\mathrm{Im}(\mathrm{E}_x \mathrm{E}_z^*) \,\mathrm{Im}(\partial_x \mathrm{G}_{xz}), \\
F_z &= \frac{1}{2}\Re(\alpha \mathbf{E} \partial_z \tilde{\mathbf{E}}^{0*}) + \frac{1}{2}|\alpha|^2 \omega^2 \mu_1 \mu_0 (|\mathrm{E}_x|^2 \Re(\partial_z \mathrm{G}_{xx}) + |\mathrm{E}_z|^2 \Re(\partial_z \mathrm{G}_{zz})).
\end{aligned} \tag{S15}
$$

As a consequence of Equation (S3), the vertical force F_z does not change sign with the beam focus tuning, Figure S1. Plasmon excitation modifies vertical force but symmetrically with respect to f.

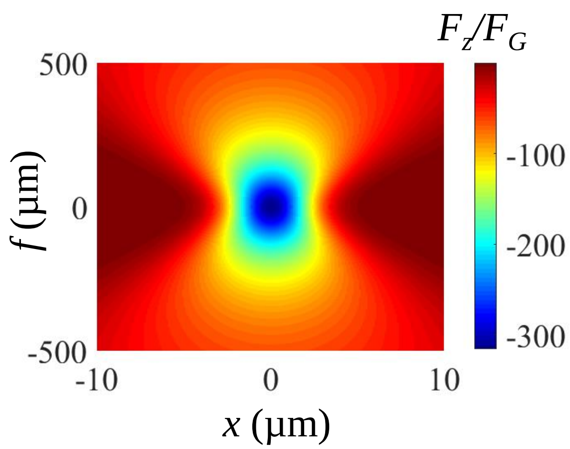

Figure S1. The same as in Figure 3 but for the vertical component of the force.

D. Transverse force at plasmon resonance

By introducing coefficient $C = \dfrac{1}{\left(1-\omega^2 \mu_1 \mu_0 G_{xx} \alpha\right)\left(1-\omega^2 \mu_1 \mu_0 G_{zz}^* \alpha^*\right)}$ the transverse force (Equation (S15)) can be written as

$$F_x = \frac{1}{2}\Re(\alpha \mathbf{E}\partial_x \tilde{\mathbf{E}}^{0*}) + |\alpha|^2 \omega^2 \mu_1 \mu_0 \operatorname{Im}(\partial_x \mathrm{G}_{xz})\left(\Re(\tilde{\mathrm{E}}_x^0 \tilde{\mathrm{E}}_z^{0*})\operatorname{Im}(\mathrm{C}) + \operatorname{Im}(\tilde{\mathrm{E}}_x^0 \tilde{\mathrm{E}}_z^{0*})\Re(\mathrm{C})\right) \quad \text{(S16)}$$

At the plasmon resonance for small z the sum of the first two terms is smaller by absolute value than the last term. Neglecting the first two terms and taking into account that $\Re(\mathrm{C}) \approx 1$ we obtain

$$F_x \approx |\alpha|^2 \omega^2 \mu_1 \mu_0 \operatorname{Im}(\partial_x \mathrm{G}_{xz}) \operatorname{Im}(\tilde{\mathrm{E}}_x^0 \tilde{\mathrm{E}}_z^{0*}) . \quad \text{(S17)}$$

E. Paraxial model for the Gaussian beam

To find the expressions for the Gaussian beam corresponding to Equations (4) in the paraxial approximation we start from the magnetic component, Figure S2:

$$\begin{gathered}\tilde{H}_y^0 = \sqrt{\frac{\varepsilon}{\mu}}\left(\frac{w}{\sqrt{c_i}} \mathrm{e}^{-ik_1(z-f)-\frac{x^2}{c_i}} + r_p \frac{w}{\sqrt{c_r}} \mathrm{e}^{ik_1(z+f)-\frac{x^2}{c_r}}\right), \\ c_i = w^2 - \frac{2i(\mathrm{z}-\mathrm{f})}{k_1}, \qquad c_r = w^2 + \frac{2i(\mathrm{z}+\mathrm{f})}{k_1}.\end{gathered} \quad \text{(S18)}$$

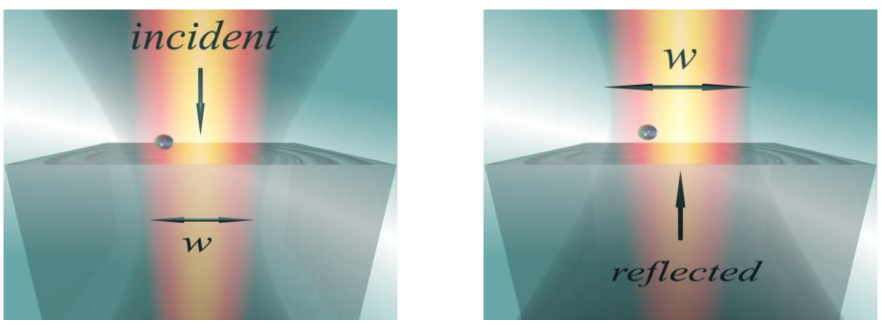

Figure S2. Incident and reflected Gaussian beams.

Here the reflection coefficient r_p is calculated in the approximation that the Gaussian beam is reflected as a normally incident plane wave with the wave vector k_1 (see Supplementary Information I2 on the validity of this approximation).

By using Maxwell's equations $E_x = -\frac{1}{ik_1}\sqrt{\frac{\mu}{\varepsilon}}\frac{\partial H_y}{\partial z}$, $E_z = \frac{1}{ik_1}\sqrt{\frac{\mu}{\varepsilon}}\frac{\partial H_y}{\partial x}$ the corresponding electric field components are

$$\tilde{E}_x^0 = \left(\frac{w}{k_1^2\sqrt{c_i}} \left(k_1^2 + \frac{2x^2}{c_i^2} - \frac{1}{c_i} \right) e^{-ik_1(z-f)-\frac{x^2}{c_i}} - r_p \frac{w}{k_1^2\sqrt{c_r}} \left(k_1^2 + \frac{2x^2}{c_r^2} - \frac{1}{c_r} \right) e^{ik_1(z+f)-\frac{x^2}{c_r}} \right),$$
$$\tilde{E}_z^0 = 2xi\frac{w}{k_1}\left(\frac{1}{c_i^{\frac{3}{2}}} e^{-ik_1(z-f)-\frac{x^2}{c_i}} + r_p \frac{1}{c_r^{\frac{3}{2}}} e^{ik_1(z+f)-\frac{x^2}{c_r}} \right). \tag{S19}$$

F. Optical potential of Gaussian beam focused on the substrate

To elucidate how optical tweezer formed by Gaussian beam focused on plasmon substrate can trap the particle, Figure S3 plots the depth of optical potential (F_x integral over x coordinate) in dependence of beam intensity. In order to achive stable optical trapping, the potential barrier should be about 10kT[1].

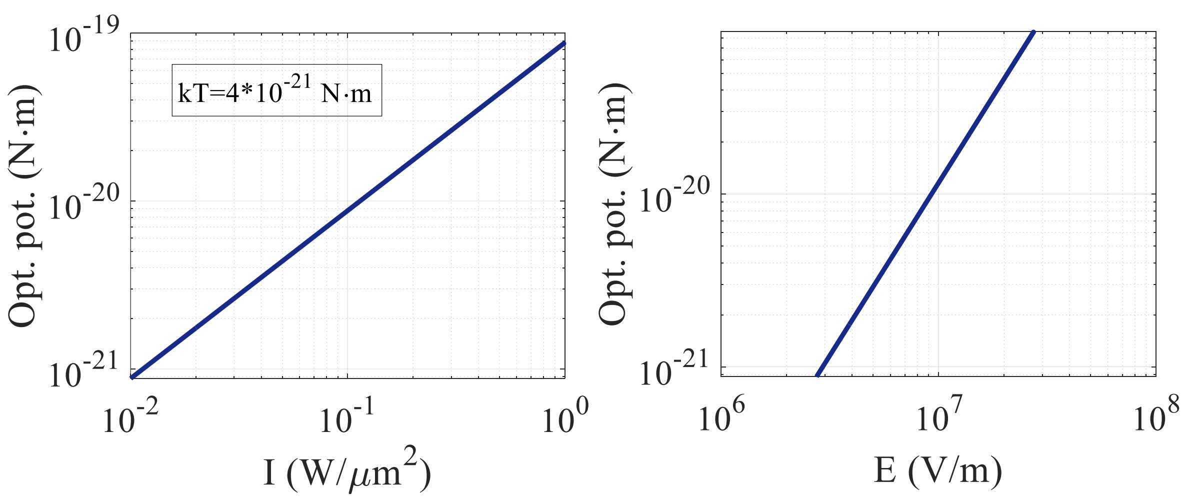

Figure S3 Optical potential (along x-direction) in Gaussian beam focused on the substrate. The beam properties: w=10λ, λ=342 nm, f=50 µm, ε_2=-1.25+0.32i, ε_1=1; the particle: ε=3, R=15 nm, z=15 nm.

To estimate realistic forces we can find radiation pressure on the particle in the middle of free-space Gaussian beam F_G which was used as a normalization value. For beam of waist 10λ (λ=342 nm) we obtain F_G approximately 6 fN/(W/µm^2). Referring to Figure 2a we obtain transversal force about 30 fN/(W/µm^2) for a particle over plasmonic substrate. Optical forces in fN-range were recently measured experimentally[2].

G. Dipole moment of the particle

In order to gain an intuitive understanding of the trapping and anti-trapping effects, the geometrical optics model can be considered. Ray tracing at different focus positions of the Gaussian beam results in essentially different pictures for the positive and negative f, Figure S4a,b. In the upper half-space, the reflected rays are directed from the beam axis in the case of the positive focus (f>0) (Figure S4a), while for f<0 they are bent towards the center of the beam (Figure S4b).

Traditionally, relative intensity of rays (without considering polarization effects which are often irrelevant in free space) is compared[3,4] and their intensification towards the beam axis predicts particle trapping what is indeed true as the bead is far from the interface. Nevertheless, near the substrate plasmon excitation changes this assessment: The polarization of interfering incident and reflected beams is different at positive and negative positions of focal plane and is the reason for plasmons to be excited with different efficiency. Differential operators in Maxwell's equations are local and allow to associate a ray in a Gaussian beam with a ray in a plane wave. Obliquely incident plane wave was studied in Ref. 5, and the picture of rays in Figure S4a could lead to plasmon-assisted motion towards the center of the beam while for Figure S4b one obtains repulsion from the beam axis.

To further reconstruct the physical picture of the effect, we deeper analyze the induced dipole moment ($\mathbf{p}$) of the particle. Non-zero phase delay $\Delta\varphi$ between p_x and p_z corresponds to the rotation of the induced dipole moment in the xz plane. Figure S4c,d shows that in the reflected Gaussian beam the vector of induced dipole moment of the particle draws an ellipse in space with time. Unidirectional rotation of the dipole compensates for the momentum taken away by plasmon and leads to the particle motion towards or from the beam axis. Improvement or reduction of trapping correlates with the value of the phase delay $\Delta\varphi$[5,6], compare $\Delta\varphi$=0.15π for f=100 µm versus $\Delta\varphi$=0.3π for f=-100 µm, Figure S4c, and corresponding F_x-F_{x0} from Figure 3. Depending on the focus position, $\Delta\varphi$ changes, taking smaller value for the negative focus compared to the positive focus, Figure S4d.

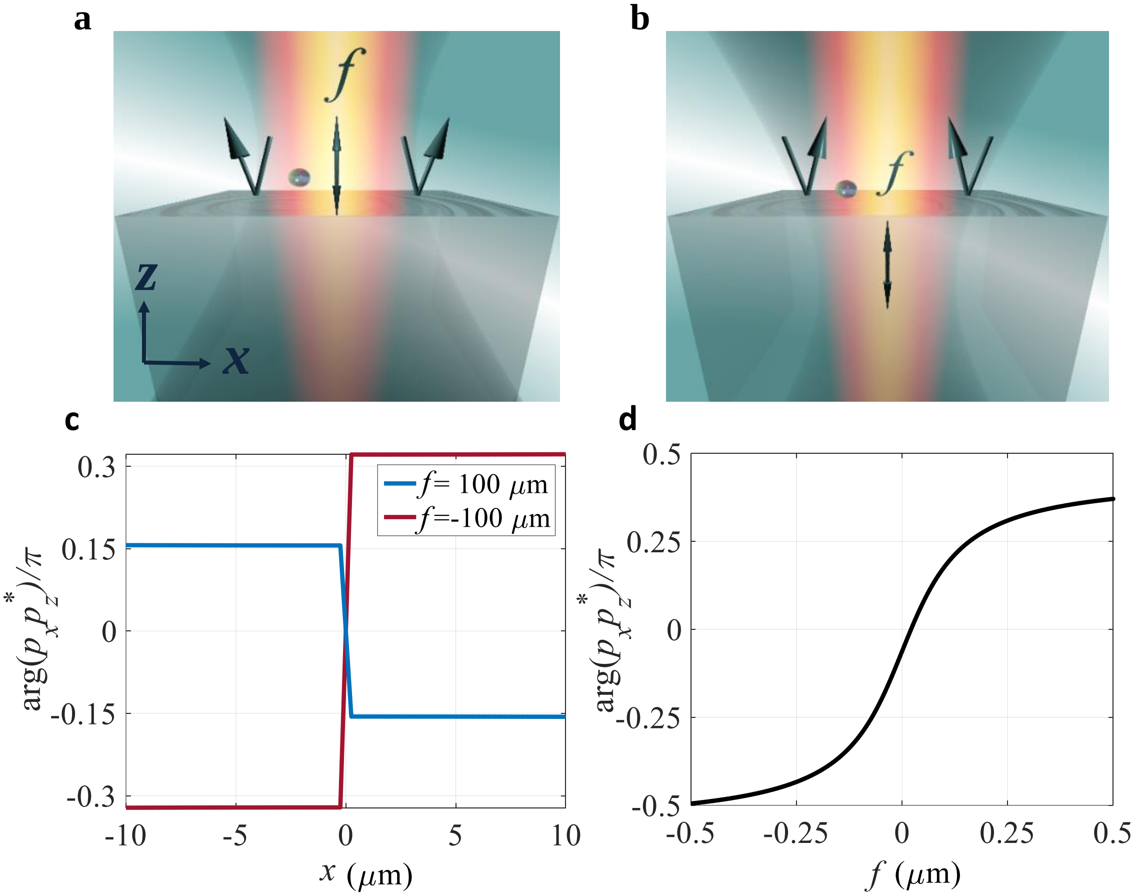

Figure S4. Interaction of Gaussian beam with a substrate, ray optics analysis. The rays diverge from the beam axis if the beam is focused above the substrate ($f>0$) (**a**), while for $f<0$ rays converge towards the center of the beam (**b**). (**c**) Phase lag between components of a dipole moment induced on a particle $p_x p_z^*$ as a function of particle position in the Gaussian beam focused on metal for two focus detunings (in the legend). (**d**) Phase lag between components of the induced dipole moment as a function of the focal position. The beam: w=10λ, λ=342 nm, ε_2=-1.25+0.32i, ε_1=1; the particle: ε=3, R=15 nm, z=15 nm.

H. FEM simulation

In Figure S5 FEM simulation is overlaid with the results of analytical model for a range of focus positions. While good match is visible for positive focus, for negative focus numerical simulation predicts more pronounced antitrapping. The reason for the discrepancy is the approximation of a point dipole for a finite-size particle, and besides finite element solution can deviate from the exact result for substrate-mediated resonance effect, e.g., spurious excitation of plasmon might happen from computational domain boundaries or mesh imperfections.

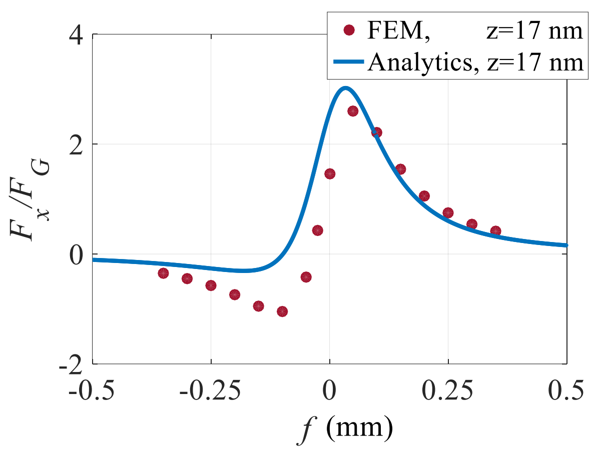

Figure S5. Transversal force F_x in the beam focused on metal substrate as calculated by analytical formalism and Comsol simulation. The beam: w=10λ, λ=342 nm, ε_2=-1.25+0.32i, ε_1=1; the particle: ε=3, R=15 nm, z=17 nm, x=-700 nm.

I. Optical forces in the paraxial approximation

1. **Lateral force F_x and term** $\mathrm{Im}(\tilde{E}_x^0\tilde{E}_z^{0*})$

To see how $F_x(f)$ transforms as the beam width w is changed, we can use approximate expression for F_x, Equation (S17)) and analyze $\mathrm{Im}(\tilde{E}_x^0\tilde{E}_z^{0*})$ which can be explicitly written in the paraxial approximation. To envisage how the expression $\mathrm{Im}(\tilde{E}_x^0\tilde{E}_z^{0*})$ changes for a dipole positioned on the metal surface close to the beam axis (then force F_x directly characterizes stiffness), for simplicity of derivation we make several assumptions.

1.1. Approximation of the field on the surface

The dipole is lying on the substrate so that *z*=0 and *x* is small: $x<\lambda<<w$. Then $c_i = c_r = w^2 c$ and $\left(k_1^2 + \frac{2x^2}{w^4c^2} - \frac{1}{w^2c}\right) \approx k_1^2 - \frac{1}{w^2c}$. Now we can obtain

$$\tilde{E}_x^0 = \frac{1}{k_1^2\sqrt{c}}\left(k_1^2 - \frac{1}{w^2c}\right)(1-r_p)\,\mathrm{e}^{ik_1 f},$$
$$\tilde{E}_z^0 = \frac{2xi}{k_1 w^2 c^{\frac{3}{2}}}(1+r_p)\,\mathrm{e}^{ik_1 f}, \qquad c = 1 + \frac{2if}{k_1 w^2}. \tag{S20}$$

This allows to find the extremum of the function $\mathrm{Im}(\tilde{E}_x^0\tilde{E}_z^{0*})$ as

$$f_\pm = \frac{b \pm \sqrt{D}}{16 k_1\,\mathrm{Im}(\mathrm{r}_p)},$$
$$b = -3(1-|\mathrm{r}_p|^2)(\mathrm{k}_1^2\mathrm{w}^2-1), \qquad \mathrm{D} = 32\,\mathrm{k}_1^4\mathrm{w}^4\,\mathrm{Im}(\mathrm{r}_p)^2 + b. \tag{S21}$$

By further simplifying (S21) we can obtain

$$f_\pm = \frac{kw^2}{16\,\mathrm{Im}(\mathrm{r}_p)}\left(3(|\mathrm{r}_p|^2-1) \pm \sqrt{32}\,\mathrm{Im}(\mathrm{r}_p)\right). \tag{S22}$$

1.2. Approximation of small focus value

For *f* being small ($f<\lambda<<w$) we can make further approximation: $\left(k_1^2 - \frac{1}{w^2c}\right) \approx k_1^2$. By using approximate expression on the basis of Taylor expansion for small *s*, $\frac{1}{(1+is)^n} \approx 1 - ins$, we can write $\frac{1}{c^n} \approx 1 - \frac{2if}{k_1 w^2}$. By plugging this into Equation (S20) in the approximation of small focus for the field on the surface one can obtain:

$$\mathrm{Im}(\tilde{E}_x^0\tilde{E}_z^{0*}) = -\frac{2x}{k_1 w^2}(1-|\mathrm{r}_p|^2) - \frac{8x\,\mathrm{Im}(r_p)}{(k_1 w^2)^2} f \quad . \tag{S23}$$

This expression allows to find zero of the function $\mathrm{Im}(\tilde{E}_x^0 \tilde{E}_z^{0*})$:

$$f_0 = -\frac{kw^2}{4\,\mathrm{Im}(\mathrm{r}_p)}(1-|\mathrm{r}_p|^2)\,. \qquad \text{(S24)}$$

1.3. Conclusion

Both focal spot positions corresponding to the maximum and minimum values of trap strength given by Equation (S22) and the threshold value of the focus where anti-trapping begins, Equation (S24), scale with the beam size as w^2, which is in line with the estimations from the exact analytical model. The value of $\mathrm{Im}(\tilde{\mathrm{E}}_x^0 \tilde{\mathrm{E}}_z^{0*})$ at the points of the extremum $f_\pm$ is inversely proportional to the beam waist, and the stiffness drops for loosely focused beams.

2. Analysis of the field

In Figure S6a the product $\mathrm{Im}(\tilde{E}_x^0 \tilde{E}_z^{0*})$ is calculated according to different approaches: full non-paraxial model (Equation (4)), paraxial approach assuming Gaussian beam reflected as a plane wave (Equations (S19)) and paraxial approximation for small x and z (Equations (S20)). The approaches give negligible difference and the force calculation appears to be robust in regards to field definition.

To further study the field effect starting from the very basics, let's consider incident field, i.e. a free space Gaussian beam at small x:

$$E_z^{inc} = \bar{E}_z^{inc}\,\mathrm{e}^{ik_1 f} = 2xi\frac{w}{k_1}\frac{1}{c_i^{\frac{3}{2}}}\mathrm{e}^{ik_1 f}\,. \qquad \text{(S25)}$$

Here we suppose that the observation point is fixed in space while the free-space Gaussian beam is shifted. Since the phase factor $\mathrm{e}^{ik_1 f}$ does not play any role in $\mathrm{Im}(\tilde{E}_x^0 \tilde{E}_z^{0*})$ evaluation, we plot $\Re(\bar{E}_z^{inc})$ in Figure S6b which changes asymmetrically with focus.

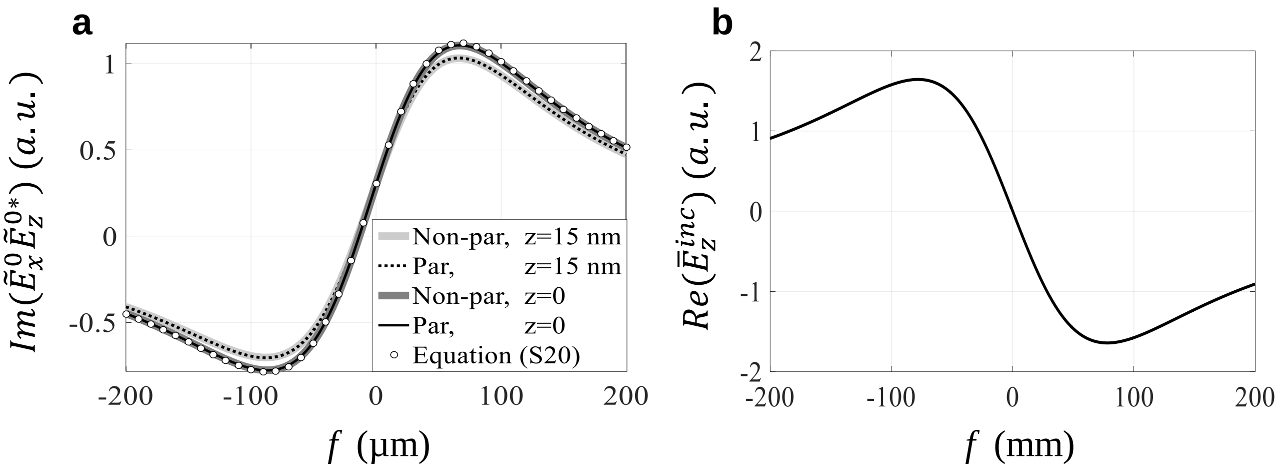

Figure S6. (**a**) Comparison of the $\mathrm{Im}(\tilde{E}_x^0\tilde{E}_z^{0*})$ evaluated according to the different approaches shows the validity of the paraxial approximation. Beam waist is w=10λ, λ=342 nm, x=-300 nm, ε_2=-1.25+0.32i, ε_1=1. The particle (ε=3, R=15 nm) is positioned at x=-300 nm, z=15 nm. (**b**) Incident field $\bar{E}_z^{inc}$ component defined according Equation (S25) at x=-300 nm for w=10λ, λ=342 nm.

References

1 Ashkin A, Dziedzic JM, Bjorkholm JE, Chu S. Observation of a single-beam gradient force optical trap for dielectric particles. *Opt Lett* 1986; **11**: 288–290.

2 Shilkin DA, Lyubin EV, Soboleva IV, and Fedyanin AA. Direct measurements of forces induced by Bloch surface waves in a one-dimensional photonic crystal. Opt Lett 2015, **40**: 4883–4886.

3 Novotny L, Hecht B. *Principles of Nano-Optics*. 2nd edn. New York: Cambridge University press; 2012.

4 Ashkin A. Forces of a single-beam gradient laser trap on a dielectric sphere in the ray optics regime. *Biophys J* 1992; **61**: 569–582.

5 Petrov MI, Sukhov SV, Bogdanov AA, Shalin AS, Dogariu A. Surface plasmon polariton assisted optical pulling force. *Laser Photonics Rev* 2016; **122**: 116–122.

6 Rodríguez-Fortuño FJ, Marino G, Ginzburg P, O'Connor D, Martínez A *et al.* Near-field Interference for the Unidirectional Excitation of Electromagnetic Guided Modes. *Science* 2013; **340**: 328–330.